

Supplemental information

TET2 is a component of the estrogen receptor complex and controls 5mC to 5hmC conversion at estrogen receptor *cis*-regulatory regions

Rebecca Broome, Igor Chernukhin, Stacey Jamieson, Kamal Kishore, Evangelia K. Papachristou, Shi-Qing Mao, Carmen Gonzalez Tejedo, Areeb Mahtey, Vasiliki Theodorou, Arnoud J. Groen, Clive D'Santos, Shankar Balasubramanian, Anca Madalina Farcas, Rasmus Siersbæk, and Jason S. Carroll

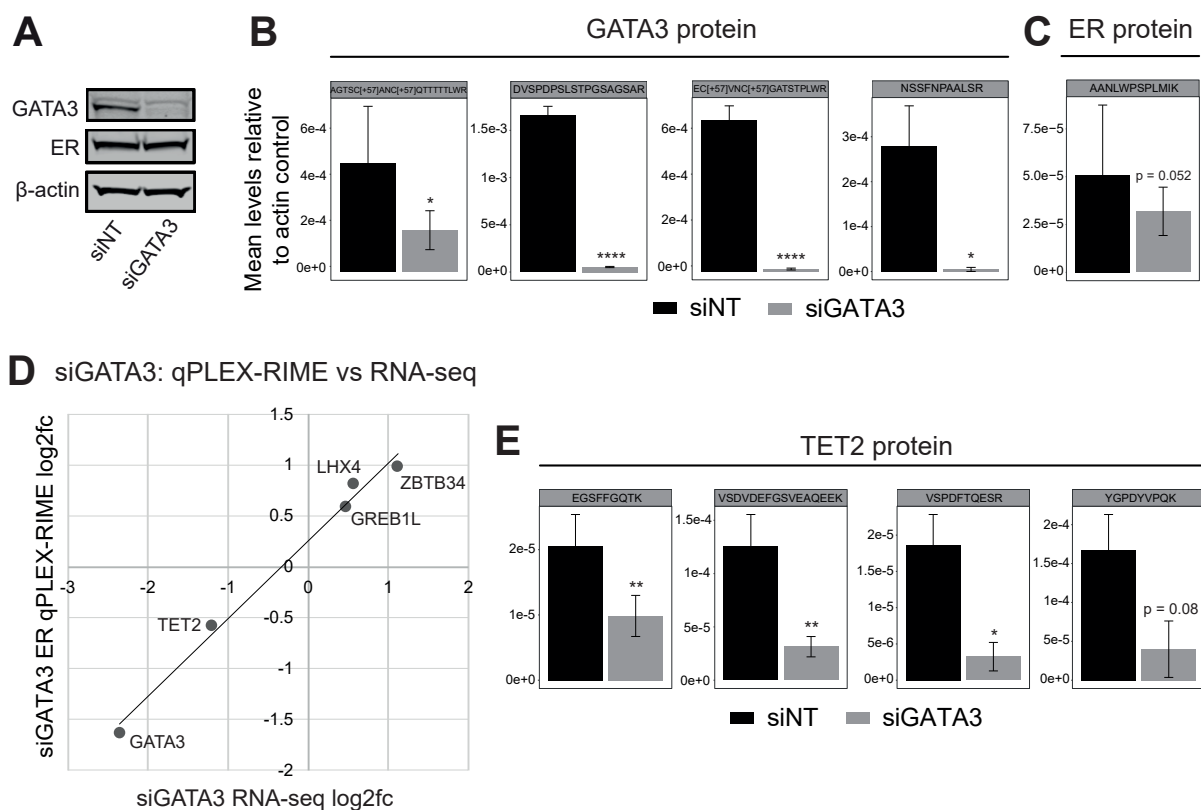
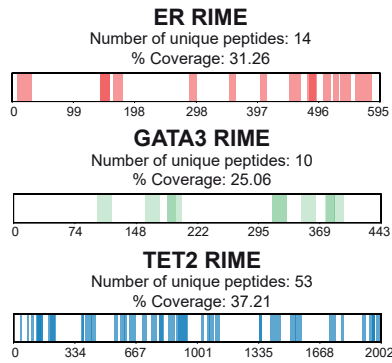


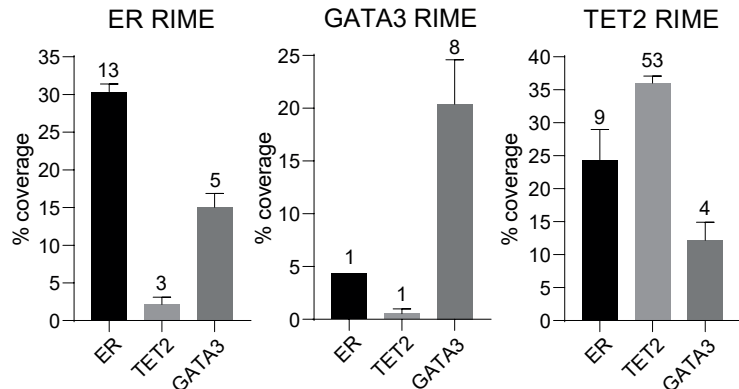
Figure S1. Western blot and PRM confirm effective GATA3 knockdown, and RNA-seq demonstrates that proteomic changes to the ER complex are paralleled at the RNA level for all significantly altered targets, and additionally at the protein level for TET2 (related to Figure 1).

A) Western blot for GATA3 and ER after 48 hours' treatment with either non-targeting control siRNA (siNT) or siRNA targeting GATA3 (siGATA3), demonstrating robust GATA3 depletion with no effect on total ER levels. β -actin is used as a loading control. B) PRM results showing levels of different GATA3 peptides or C) the single ER peptide detected, respectively, in response to siNT or siGATA3 treatment (48 hours). D) Correlation between log2 fold change values obtained for selected targets in ER qPLEX-RIME versus RNA-seq upon GATA3 knockdown. E) PRM results showing levels of different TET2 peptides in response to siNT or siGATA3 treatment (48 hours). All PRM results represent mean \pm SD peptide levels relative to an actin control (n = 3). ** = $p \leq 0.01$, **** = $p \leq 0.0001$.

A RIME coverage diagrams



B RIME % coverage and unique peptides



C

ER, TET2 and GATA3 common interactors from RIME

ACIN1	DAZAP1	GATA3	LUC7L	PRDX1	RPL17	SF3B4	TKT
ACP1	DBR1	GATAD2B	LUC7L2	PRKDC	RPL21	SLC9A3R1	TLE1
ACTC1	DCAF7	GMPS	LUC7L3	PRMT1	RPL22	SLTM	TLE3
ADAR	DDB1	GRB2	MATR3	PRMT6	RPL24	SMARCA4	TLK2
AES	DDX1	GREB1	MBNL2	PRPF19	RPL27	SMARCB1	TMPO
AHCY	DDX17	GRHL2	MCM3	PRPF3	RPL3	SMARCC1	TNPO1
AHDC1	DDX21	GTF2I	MCM7	PRPF31	RPL34	SMARCC2	TPM4
AKAP8	DDX23	H1FO	MEMO1	PRPF38B	RPL35	SMARCD2	TPR
AKAP8L	DDX39B	H2AFY	MFAP1	PRPF4	RPL35A	SMARCE1	TRA2A
API5	DDX3X	H2AFZ	MLF2	PRPF6	RPL4	SMC1A	TRA2B
ARF3	DDX42	HDAC2	MOV10	PRPF8	RPL6	SMU1	TRIM24
ARGLU1	DDX46	HIST1H2AB	MTA2	PSPC1	RPL7	SNRNP200	TRIM25
ARID1A	DDX5	HIST1H2BJ	MYEF2	PTBP1	RPRD2	SNRNP40	TRIM28
ARID1B	DDX6	HIST1H3A	MYH14	PTBP3	RPS10	SNRPA1	TRIM33
ARL6IP4	DHX15	HMCE5	MYH9	PUF60	RPS11	SNRPB	TRIP6
BCL9L	DKC1	HMGB2	MYL6	QKI	RPS13	SNRPD1	TRPS1
BCLAF1	DNAJA1	HMGB3	NACC1	RACK1	RPS14	SNRPD2	TUBB
BOLA2	DNAJB1	HNRNPA0	NAT10	RAI1	RPS15	SNRPE	U2AF1
BUB3	DYNLL1	HNRNPAB	NCBP1	RALY	RPS15A	SNW1	U2AF2
CARM1	EEF1D	HNRNPC	NCBP2	RAN	RPS16	SRRM1	U2SURP
CBX3	EEF2	HNRNPD	NCOA3	RARA	RPS2	SRRM2	UBAP2L
CBX5	EFTUD2	HNRNPDL	NCOA5	RBBP7	RPS20	SRRT	UBC
CCAR1	EIF3I	HNRNPF	NCOR1	RBM10	RPS21	SRSF1	UGDH
CCAR2	EIF4A1	HNRNPH2	NCOR2	RBM12	RPS24	SRSF10	UPF1
CDC5L	EIF4A3	HNRNPH3	NKRF	RBM12B	RPS25	SRSF5	USP39
CEBPB	EIF4B	HNRNPL	NMD3	RBM14	RPS27	SRSF6	XPO1
CELF1	EIF4H	HNRNPLL	NONO	RBM15	RPS28	SRSF7	XRCC5
CFL1	EIF5A	HNRNPM	NOP58	RBM22	RPS3A	SRSF9	XRCC6
CHERP	ELAVL1	HNRNPR	NR2F2	RBM25	RPS4X	SSB	XRN2
CIRBP	ENO1	HNRNPU	NRIP1	RBM3	RPS7	SSRP1	YLPM1
CLIC3	ERH	HNRNPUL1	NUDT16L1	RBM33	RPS9	STARD10	YTHDF2
CLK3	ESR1	HNRNPUL2	NUDT21	RBM39	RSRC2	STAT3	YWHAQ
CLTC	ESRP1	HSP90AA1	NUMA1	RBM4	RTCB	STAU1	ZC3H11A
CPNE3	ESRP2	HSPA1B	NXF1	RBM45	RTFDC1	STRBP	ZC3H14
CPSF1	FAM120A	HSPA8	OGT	RBM4B	RXRA	SUB1	ZC3H18
CPSF6	FAM50A	ILF2	PA2G4	RBM8A	S100A11	SUMO1P1	ZC3H4
CPSF7	FAM98B	KDM1A	PABPC1	RBMX	SAFB	SUPT16H	ZFR
CREBBP	FASN	KHDRBS1	PABPN1	RBPMS	SAFB2	SUPT5H	ZNF207
CRIP2	FEN1	KHSRP	PARP1	RCC1	SARNP	SYNCRIP	ZNF217
CRNKL1	FIP1L1	KPNA2	PCBP1	RCC2	SART1	TAF15	ZNF281
CSDE1	FOSL2	KRT14	PCBP2	RNF20	SART3	TAGLN2	ZNF326
CSE1L	FOXA1	L1RE1	PDCD6	RNF40	SBNO2	TBL1XR1	ZNF385A
CSNK1A1	FUBP1	LARP4	PFN1	RNH1	SET	TBX2	ZNF638
CSTF1	FUBP3	LASP1	PFN2	RPL10	SF1	TCERG1	
CSTF2	FUS	LGALS3	PIAS3	RPL13	SF3A3	TCF20	
CSTF3	FXR1	LMNA	PKM	RPL13A	SF3B1	TET2	
CTBP1	G3BP1	LMNB1	POLDIP3	RPL14	SF3B2	THRAP3	
CTBP2	GAPDH	LMX1B	PPIA	RPL15	SF3B3	TIAL1	

Figure S2. ER, GATA3 and TET2 are detected as reciprocal interactors of one another using RIME, and share a large number of common interactors (related to Figure 1). A) Non-quantitative RIME in MCF7 cells yielded robust coverage of the three bait proteins ER, GATA3 and TET2, indicated by coverage diagrams showing the unique peptides identified with high confidence across the protein sequence. The number of unique peptides and corresponding % sequence coverage is shown above each plot. Each diagram provides a representative example of three biological replicates. B) Barplots depicting the % peptide sequence coverage for ER, GATA3 and TET2 in separate RIME experiments, indicating that these three proteins are reciprocally detected as interactors of one another using RIME. Results represent mean \pm SD ($n = 3$). The number of unique peptides detected for each protein (the average of three biological replicates) is indicated above each bar. C) Full list of ER/GATA3/TET2 common interactors. Specific interactors were considered as those occurring in at least two out of three independent replicates. Any proteins that appeared in any one of three IgG negative control RIME experiments were excluded.

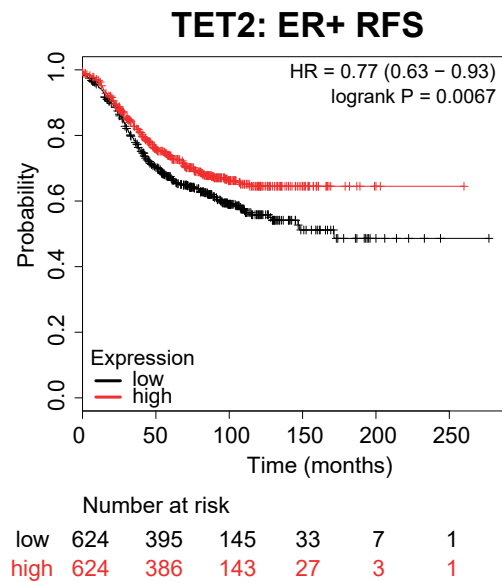


Figure S3. Higher TET2 mRNA expression is associated with improved relapse-free survival in ER+ breast cancer (related to Figure 2). Kaplan-Meier plotter-generated plot (Györfy et al. 2013) demonstrating relapse-free survival (RFS) in patients with high versus low TET2 mRNA expression. HR = hazard ratio.

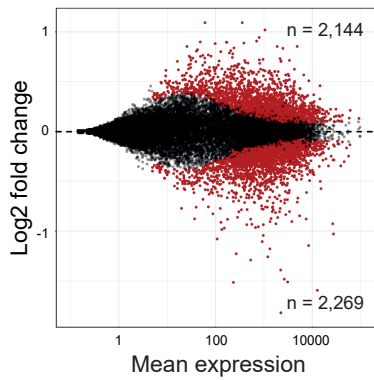
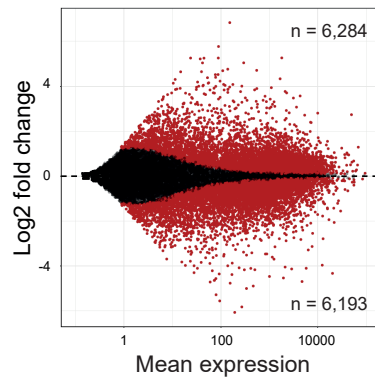
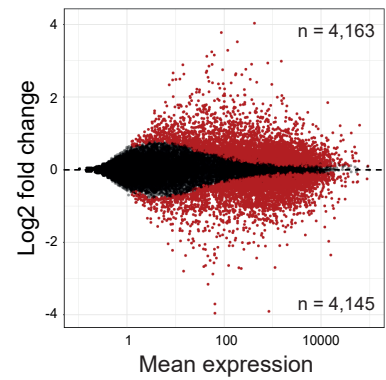
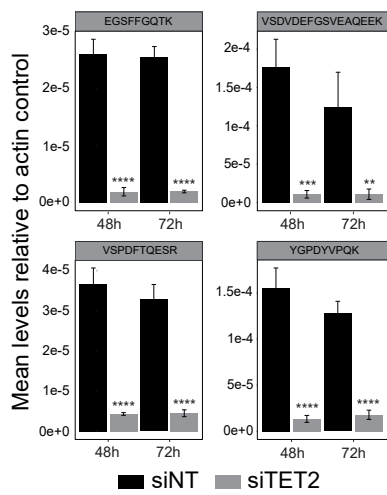
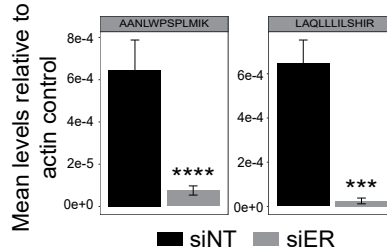
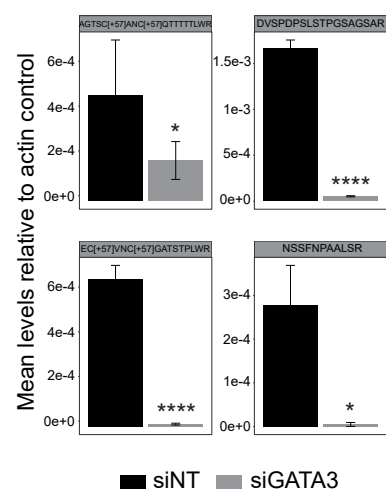
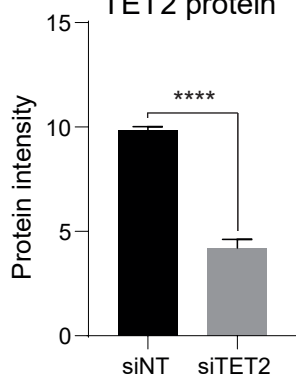
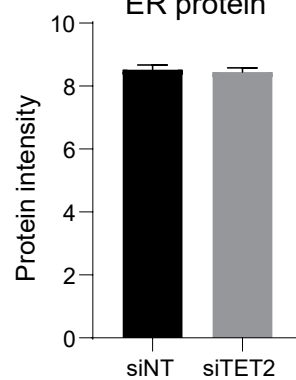
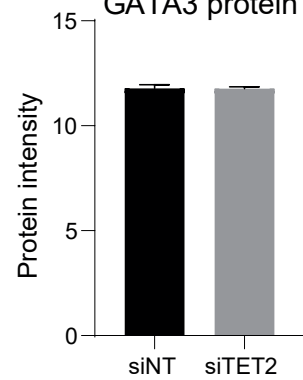
A Gene expression changes after TET2 knockdown**B** Gene expression changes after ER knockdown**C** Gene expression changes after GATA3 knockdown**D** TET2 protein**E** ER protein**F** GATA3 protein**G** TET2 protein**H** ER protein**I** GATA3 protein

Figure S4. Individual knockdown of TET2, ER and GATA3 affects gene expression in MCF7 cells, with the extent of depletion of each target protein confirmed using PRM. TET2 knockdown does not affect total ER or GATA3 protein levels according to whole proteome analysis (related to Figures 3 and 4). MA plots demonstrating gene expression changes in response to either A) siTET2, B) siER or C) siGATA3 treatment (48 hours) in MCF7 cells (n = 6). Regulated genes according to $p \leq 0.05$ are highlighted in red, with the corresponding number of genes indicated. Barplots in D), E) and F) depict protein-level validation of each knockdown using PRM, with each plot indicating an individual unique peptide. All PRM results represent mean \pm SD peptide levels relative to an actin control (n = 3). ** = $p \leq 0.01$, **** = $p \leq 0.0001$. G), H) and I) Selected results from whole proteome analysis showing TET2 (G), ER (H) and GATA3 (I) levels in response to siNT or siTET2 treatment (72 hours). Four replicates of each condition were included in an 11plex TMT MS run. Results represent mean \pm SD protein intensity, which is the aggregate of intensities of the individual unique peptides identified for each protein. **** = $p \leq 0.0001$.

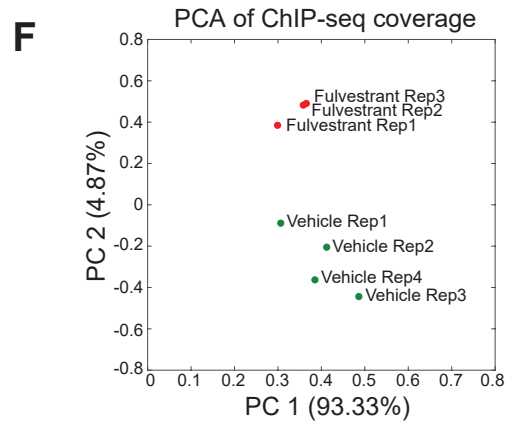
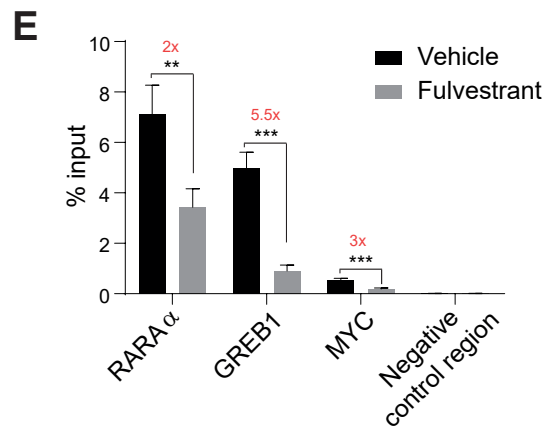
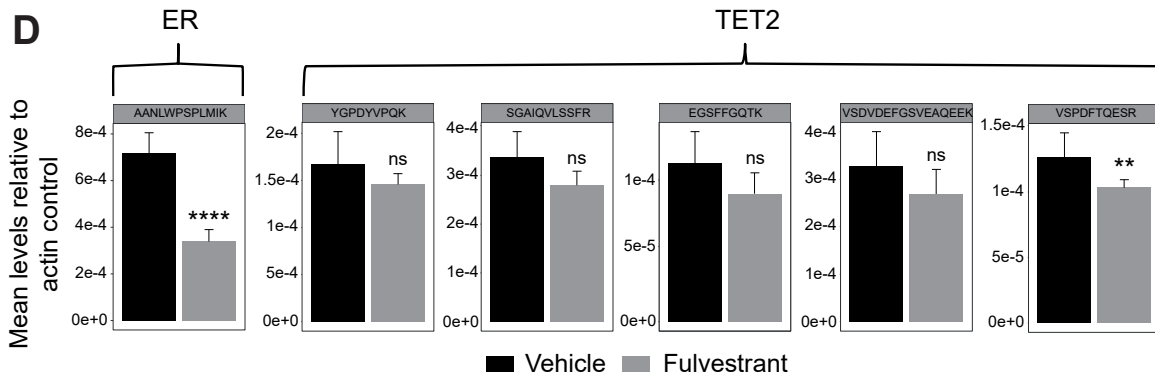
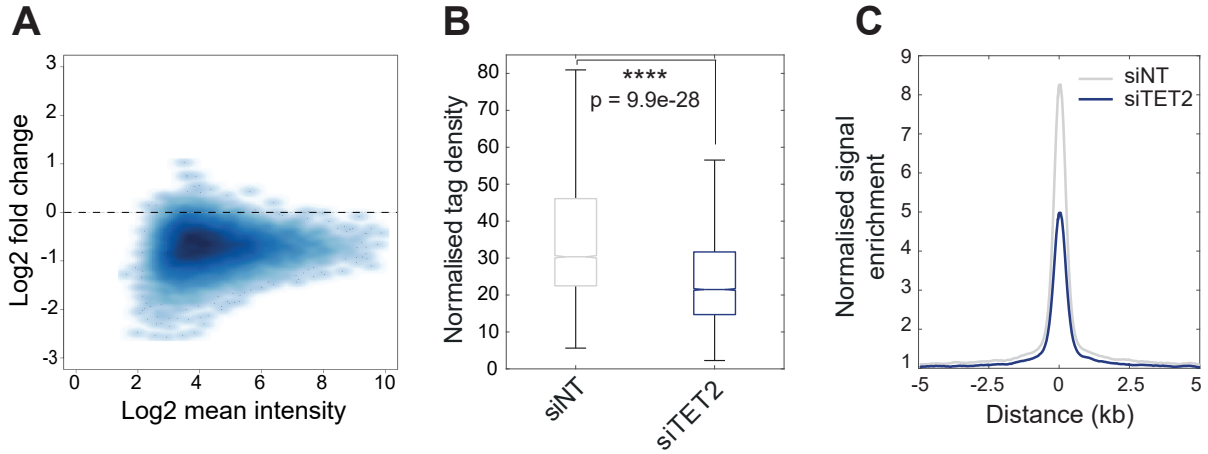


Figure S5. TET2 knockdown depletes global TET2 binding, validating the TET2 antibody (related to Figures 1, 2 and 4). Acute fulvestrant treatment significantly depletes ER protein levels concurrent with a reduction in ER chromatin occupancy at key ER enhancers, but does not dramatically impact TET2 total protein levels (related to Figure 4). A) MA plot showing log₂ fold change in TET2 binding in control (siNT) versus TET2 knockdown (siTET2) conditions against log₂ mean intensity of ChIP-seq signal for all TET2 sites (12,728 peaks). B) Boxplot showing the normalised tag density of TET2 ChIP-seq signal in siNT and siTET2-treated conditions within all TET2 peaks. **** = $p \leq 0.0001$. C) Average plot showing normalised signal enrichment of TET2 ChIP-seq under siNT or siTET2-treated conditions within all TET2 peaks. TET2 knockdown was performed for 48 hours. ChIPs were performed in biological triplicate. D) PRM results showing levels of a single unique ER peptide (left) or multiple TET2 peptides (right) in response to vehicle (ethanol, 3 hours) or fulvestrant (100 nM, 3 hours). Results represent mean \pm SD peptide levels relative to an actin control (n = 4). ** = $p \leq 0.01$, **** = $p \leq 0.0001$. E) ChIP-qPCR results showing reduction of ER chromatin occupancy in response to treatment with vehicle (ethanol, 3 hours) or fulvestrant (100 nM, 3 hours) at several key ER binding sites. Results represent mean \pm SD, n = 4. * = $p \leq 0.05$, ** = $p \leq 0.01$, *** = $p \leq 0.001$. F) Principal component analysis (PCA) plot demonstrating consistency between fulvestrant and vehicle-treated TET2 ChIP-seq replicate samples.

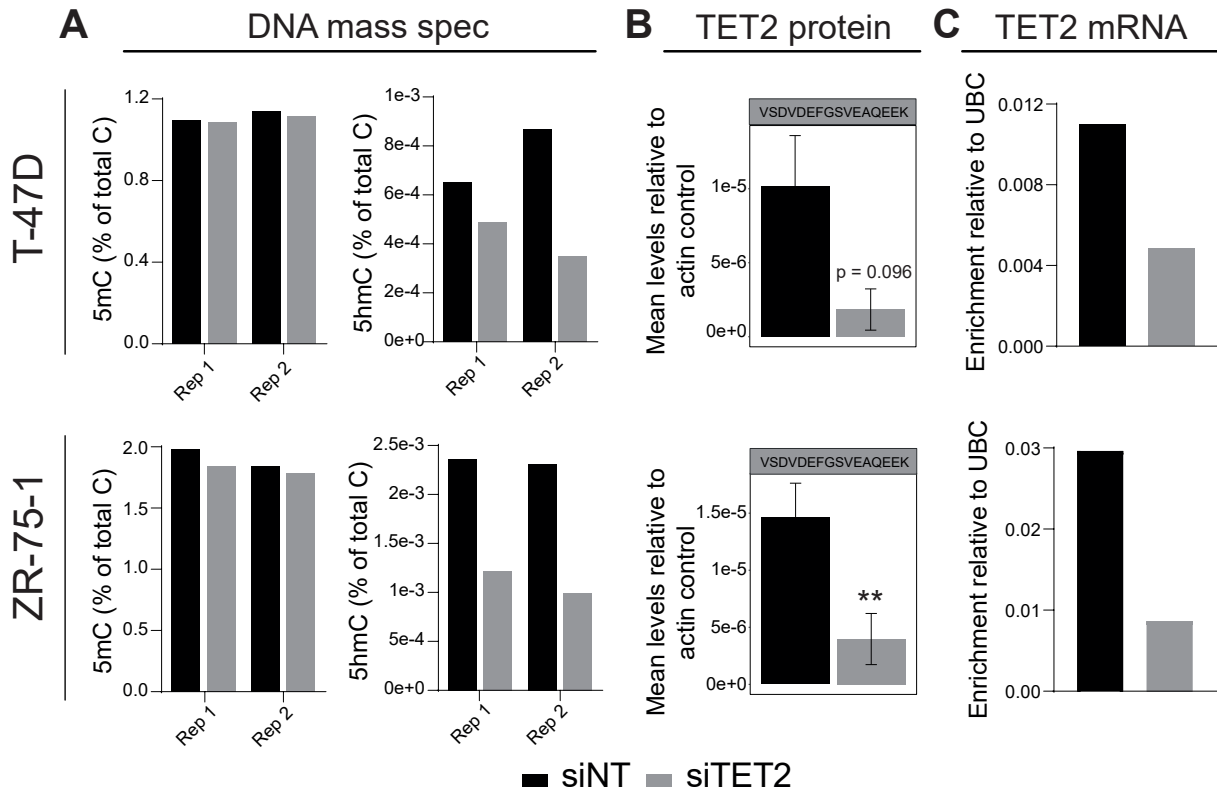


Figure S6. TET2 knockdown in T-47D and ZR-75-1 cells induces a global drop in 5hmC levels, but no change in overall 5mC levels (related to Figure 6). A) Mass spectrometry was used to assess global levels of 5mC (left) or 5hmC (right) in DNA isolated from T-47D cells or ZR-75-1 cells treated for 72 hours with either non-targeting control siRNA (siNT) or siRNA targeting TET2 (siTET2). Measurements from two independent biological replicates are plotted separately. Results are expressed as % of total cytosines. B) PRM results showing levels of the TET2 peptide VSDVDEFGSVEAQEEK in response to siNT or siTET2 treatment (72 hours) in T-47D cells (top) and ZR-75-1 cells (bottom). Results represent mean \pm SD peptide levels relative to an actin control (n = 3). ** = $p \leq 0.01$. C) To validate the TET2 knockdown further, TET2 mRNA levels in T-47D cells (top) and ZR-75-1 cells (bottom) in response to siNT or siTET2 treatment (48 hours) were assessed using qRT-PCR. Data are expressed as enrichment relative to a housekeeping control gene (UBC) (n = 1, mean of three technical replicates).